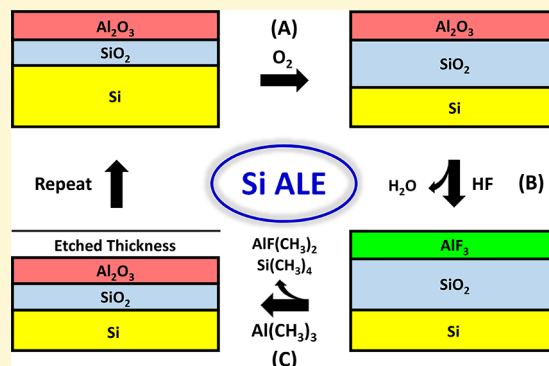


Thermal Atomic Layer Etching of Silicon Using O₂, HF, and Al(CH₃)₃ as the Reactants

Aziz I. Abdulagatov[†] and Steven M. George^{*,†,‡,§}

[†]Department of Chemistry and Biochemistry and [‡]Department of Mechanical Engineering, University of Colorado, Boulder, Colorado 80309-0215, United States

ABSTRACT: Thermal atomic layer etching (ALE) of silicon was performed using O₂, HF, and Al(CH₃)₃ as the reactants at temperatures from 225 to 290 °C. This thermal etching process is based on Si oxidation using O₂ and conversion of SiO₂ to Al₂O₃ using trimethylaluminum (TMA). Al₂O₃ is then fluorinated by HF to produce AlF₃ prior to removal of AlF₃ by a ligand-exchange reaction with TMA. Thermal Si ALE was studied using silicon-on-insulator wafers. *In situ* spectroscopic ellipsometry was employed to monitor simultaneously both the thickness of the top SiO₂ layer and the underlying silicon film during Si ALE. These studies revealed that the silicon film thickness decreased linearly with the number of reaction cycles while the thickness of the SiO₂ layer remained constant. Using an O₂–HF–TMA exposure sequence, the Si ALE etch rate was 0.4 Å/cycle at 290 °C. This etch rate was obtained using static reactant pressures of 250, 1.0, and 1.0 Torr and exposure times of 10, 5, and 5 s for O₂, HF, and TMA, respectively. The SiO₂ thickness was 10–11 Å under these reaction conditions at 290 °C. The Si ALE etch rate increased with O₂ and TMA pressure before reaching a limiting etch rate at higher O₂ and TMA pressures. The order of the reactants affected the Si etch rate. Changing the exposure sequence from O₂–HF–TMA to O₂–TMA–HF decreased the etch rate from 0.4 to 0.2 Å/cycle at 290 °C. Decreasing the etch temperature below 290 °C also resulted in a decrease in the Si etch rate. Atomic force microscopy measurements determined that the root-mean-square (RMS) roughness of the surface was 2.0 ± 0.2 Å before and after Si ALE using the optimum reaction conditions. Decreasing the static O₂ pressures below 250 Torr decreased the etch rate and also increased the RMS surface roughness. There was no evidence of any change in the Si ALE process for ultrathin Si films with thicknesses of <100 Å in the quantum confinement regime. Thermal Si ALE should be useful for silicon applications in many areas, including electronics, optoelectronics, thermoelectrics, and photonics.



I. INTRODUCTION

Atomic layer etching (ALE) is a thin film removal technique based on sequential, self-limiting surface reactions.¹ Plasma and thermal approaches exist for ALE. Plasma ALE usually involves halogenation followed by the use of energetic ions to stimulate the desorption of halide surface species.¹ The directional nature of the ions leads to anisotropic etching. Plasma ALE has been demonstrated for Si,^{2–5} Ge,⁶ and various compound semiconductors.^{7,8} Plasma ALE has also been reported for various oxides and nitrides such as SiO₂,^{9,10} HfO₂,^{11,12} and Si₃N₄.^{13,14} Other plasma ALE studies have been performed on different carbon substrates.^{15,16}

Silicon plasma ALE has been accomplished using either Cl or F adsorption that was subsequently followed by the removal of silicon halides using Ar⁺ ion bombardment.^{2–4} Alternative approaches for Si ALE utilize energetic neutral Ar beam bombardment.⁵ During the ion etching step, control of the incident ion energies is required such that the surface is exposed to ions with energies greater than the sputtering threshold of the halogenated surface layer but below the sputtering threshold of the underlying material. This energy

window is only 10–25 eV for silicon depending on the incident ion angle.¹⁷

Recently, thermal ALE processes have emerged as an alternative approach for ALE.^{18,19} Thermal ALE does not require the use of plasma or control of ion energies. The chemistry during thermal ALE relies on temperature and thermochemically favorable reactions to remove surface species. Thermal ALE will yield isotropic etching because the gas reactants have no preferred directionality. Many systems have been demonstrated for thermal ALE such as Al₂O₃,^{18,20–23} AlF₃,²⁴ HfO₂,^{25,26} ZrO₂,²⁷ SiO₂,²⁸ ZnO,²⁹ TiO₂,³⁰ TiN,³¹ WO₃,³² W,^{32,33} and AlN.³⁴

The first thermal ALE procedures were based on the fluorination and ligand-exchange mechanism.^{18–20,35} For thermal ALE of Al₂O₃ using HF and TMA, HF forms a thin AlF₃ surface layer on the Al₂O₃ substrate.^{20,21} Subsequently, in a ligand-exchange reaction, TMA accepts F from the AlF₃ surface layer and donates CH₃ to the AlF₃ surface layer to

Received: June 28, 2018

Revised: November 5, 2018

Published: November 5, 2018

produce volatile $\text{AlF}(\text{CH}_3)_2$ reaction products.²⁰ The overall fluorination and ligand-exchange reaction is $\text{Al}_2\text{O}_3 + 4\text{Al}(\text{CH}_3)_3 + 6\text{HF} \rightarrow 6\text{AlF}(\text{CH}_3)_2 + 3\text{H}_2\text{O}$.²⁰ This reaction mechanism is supported by *in situ* quartz crystal microbalance (QCM) and Fourier transform infrared (FTIR) vibrational spectroscopy studies.^{20,21}

The “conversion-etch” mechanism was developed to expand the number of materials that can be etched by thermal ALE processes.^{28,29} During the “conversion-etch” mechanism, the surface of the substrate is first converted to a different material that has accessible etching pathways. The conversion reaction is driven by the thermochemical stability of the different material. For example, SiO_2 ALE was initially not possible at low reactant pressures using HF and TMA.²⁷ However, at higher TMA pressures, TMA could convert SiO_2 to Al_2O_3 by reactions such as $1.5\text{SiO}_2 + 4\text{Al}(\text{CH}_3)_3 \rightarrow 2\text{Al}_2\text{O}_3 + 3\text{Si}(\text{CH}_3)_4$.²⁸ This reaction is thermochemically favorable with $\Delta G^\circ = -200$ kcal/mol at 200 °C.³⁶ The Al_2O_3 layer could then be etched using the fluorination and ligand-exchange mechanism.²⁸

Elemental materials present special challenges for thermal ALE because they are generally in the incorrect oxidation state to lead to stable, volatile etch products. Oxidation of the elemental material to an oxide can change the oxidation state of the elemental material to an oxidation state that can lead to volatile etch products. In addition, metal oxides can also be converted to different metal oxides that have accessible etching pathways. For example, W ALE was enabled by the oxidation and “conversion-etch” mechanism.³² In a three-step ABC exposure sequence, the W surface was first oxidized to a WO_3 layer using O_2/O_3 . Subsequently, the WO_3 layer was converted to B_2O_3 using BCl_3 , HF was then able to spontaneously etch the B_2O_3 surface layer.³²

In this work, thermal atomic layer etching (ALE) of silicon was performed with an oxidation and “conversion-etch” mechanism using O_2 , HF, and $\text{Al}(\text{CH}_3)_3$ as the reactants. This three-step ABC mechanism during steady state is displayed schematically in Figure 1. During this process, the Si surface is oxidized to a silicon oxide layer using O_2 . The

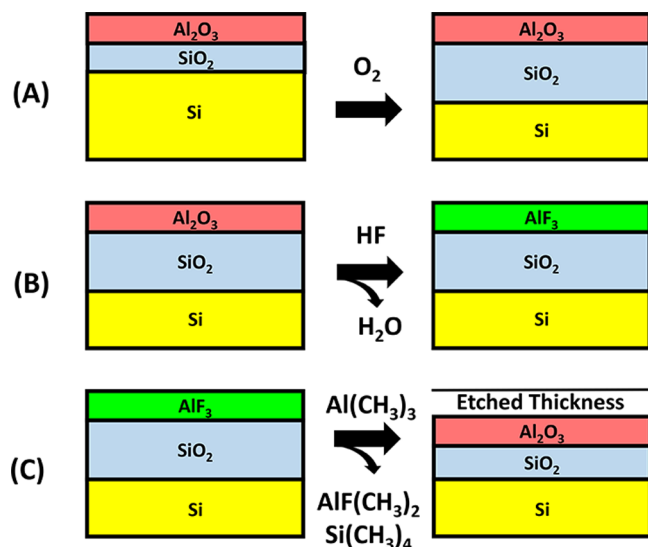


Figure 1. Schematic for thermal Si ALE based on (A) oxidation by O_2 , (B) fluorination by HF, and (C) ligand-exchange and conversion by $\text{Al}(\text{CH}_3)_3$.

silicon oxide layer is converted to an Al_2O_3 layer using trimethylaluminum (TMA).²⁸ The Al_2O_3 layer is fluorinated to an AlF_3 layer by hydrofluoric acid (HF).²⁰ The TMA can then remove this AlF_3 layer by a ligand-exchange reaction prior to converting additional SiO_2 to Al_2O_3 .²⁰ Figure 1 shows Si ALE during steady state when an Al_2O_3 layer is present on the surface after the TMA exposures. There may also be a SiO_2 layer under the Al_2O_3 layer after the TMA exposures. The O_2 exposures oxidize the silicon surface through this thin oxide layer.

This thermal Si ALE process could be important for the fabrication of advanced semiconductors.³⁷ Thermal Si ALE should produce isotropic etching that is not dependent on a line of sight to the sample. Thermal Si ALE should be able to tune precisely the thickness of silicon films on three-dimensional or complex substrates. Si ALE may be useful in silicon areas such as optoelectronics,³⁸ photonics,³⁹ thermoelectrics,⁴⁰ flexible electronics,⁴¹ microelectromechanical systems (MEMS),⁴² and ultrathin separation membranes.⁴³ Si ALE could also be valuable for the atomic-scale polishing and atomic layer cleaning of silicon substrates.

II. EXPERIMENTAL SECTION

Thermal ALE of silicon was performed in a warm wall reactor with a hot sample stage as shown in Figure 2. Figure 2a shows a cross-sectional view, and Figure 2b displays a three-dimensional (3D) perspective. The gases flow through the reactor from right to left. The reactor walls were held at 160 °C at all times. The reactor was pumped with a mechanical pump (Alcatel Adixen 2010C1). The base

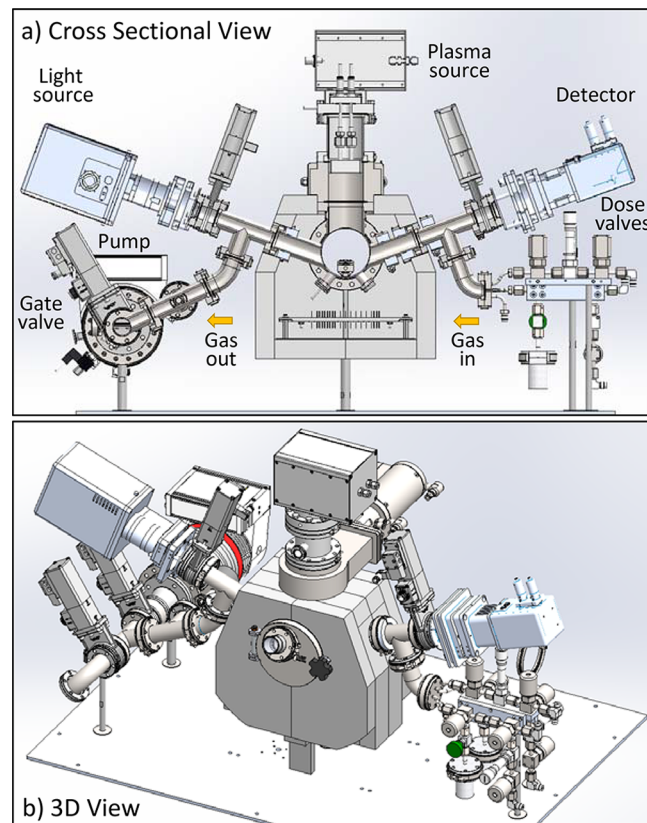


Figure 2. Warm wall reactor with a hot sample stage equipped with *in situ* spectroscopic ellipsometry used for Si ALE experiments: (a) cross-sectional view and (b) 3D perspective.

pressure of the reactor was maintained at 1 Torr with a constant flow of UHP grade N_2 gas (99.9999%, Airgas) at 100 SCCM.

The etching was studied at sample temperatures varying from 225 to 290 °C. Sample stage heating was performed using a cartridge heater. The sample was placed on the sample stage and held in place by gravity only. The sample temperature was calibrated relative to the sample stage temperature. When the sample was at 290 °C, the sample stage was at 310 °C. There was no effect of gas pressure on the sample temperature for O_2 pressures from 30 to 250 Torr.

The reactor was equipped with a mass spectrometer for gas analysis and leak checking (Stanford Research Systems RGA-200). A turbomolecular pump (Pfeiffer HiPace 300 C) was used to pump the mass spectrometer and could also pump the reactor for leak checking. The reactor also contained a plasma source (Meaglow hollow cathode plasma) on top of the reactor. Si ALE could be achieved using an O_2 plasma as the oxidation source. However, the Si ALE process using an O_2 plasma was not optimized after the determination that thermal oxidation using O_2 was sufficient to achieve Si ALE.

Two sets of boron-doped SOI wafers were used as substrates. One of the SOI samples had a 70 nm thick Si layer on a 2000 nm SiO_2 buried oxide (BOX) (University Wafer). The second SOI sample had a 100 nm thick Si (100) layer on a 200 nm SiO_2 BOX (University Wafer). All the Si ALE results presented herein, except for the experiments performed using ultrathin silicon films, were obtained using the initial 70 nm thick Si layer. The different SOI wafers yielded equivalent results. The SOI wafers were precut to 2.5 cm \times 2.5 cm coupons before use. The thermal SiO_2 ALE experiments were performed using a 80 nm thick thermal SiO_2 layer prepared by oxidation of Si(100) using H_2O (University Wafer).

The reactor was also equipped with a spectroscopic ellipsometer (J. A. Woollam M-2000UI) for *in situ* monitoring of film thicknesses at an incidence angle of 70°. The ellipsometer has a spectral range of 245–1690 nm. All film thicknesses reported in the paper were obtained using spectroscopic ellipsometry (SE). A schematic showing the film stack and ellipsometer optical beams is depicted in Figure 3. The following fitting layers from J. A. Woollam (JAW)

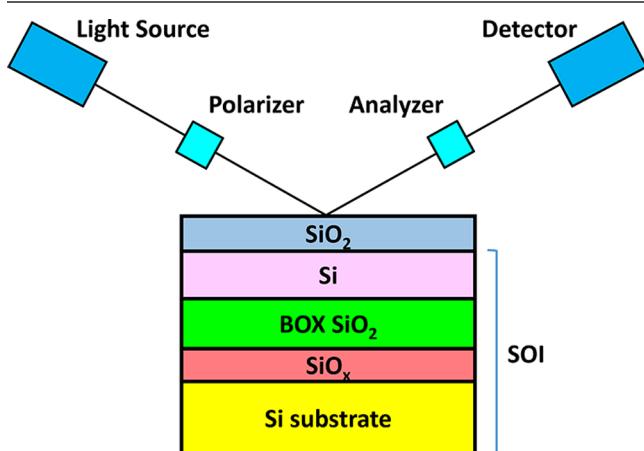


Figure 3. Ellipsometer beam interacting with a film stack on a silicon-on-insulator (SOI) wafer. The film stack is comprised of a SiO_2 layer, a Si layer, SiO_2 buried oxide (BOX), interfacial oxide, and an underlying Si substrate.

were used to model the silicon film thickness changes: SiO_2_JAW (SiO_2)/B-Spline (Si)/ SiO_2_JAW (BOX SiO_2)/INTRA_JAW (Si- SiO_2 interface layer)/Si Temp JAW (Si substrate). These fitting layers are part of the standard JAW instrument package. This modeling was performed using the CompleteEASE (J. A. Woollam) analysis software.

Data were acquired by fixing the thickness of the BOX oxide and the underlying substrate and letting the top layers SiO_2_JAW (SiO_2) and B-Spline (Si) be variable components. In the modeling of the

ultrathin silicon thicknesses, B-spline (Si) was replaced with Si Temp JAW. The ellipsometer scan time was 5 s. The Al_2O_3 layer shown in Figure 1 is not displayed in Figure 3 or included explicitly in the model. The Al_2O_3 layer is too thin for ellipsometric analysis and is treated as part of the top SiO_2 layer thickness. The SE results were recorded after the HF exposures. However, the results obtained after the various exposures within one ALE cycle during steady state SiO_2 ALE were nearly equivalent.

Thermal Si ALE was performed using O_2 , HF, and TMA as the reactants. Thermal SiO_2 ALE was performed using TMA and HF as reported previously.²⁸ Trimethylaluminum (97%) and HF, derived from HF-pyridine (70 wt %), were purchased from Sigma-Aldrich. The typical ALE cycle consisted of static exposures of O_2 for 10 s and static exposures of HF and TMA for 5 s. These exposures were all followed by 30 s N_2 purges. The N_2 purge times of 30 s were sufficient for the pressure to return to the background pressure. Industrial grade oxygen was used as the oxygen source (Airgas). All precursors were held at room temperature during the ALE and oxidation experiments. During the Si oxidation experiments, one cycle consisted of a 10 s static O_2 exposure followed by a 30 s N_2 purge.

No special precleaning procedures were applied to clean the SOI wafers or the thermal SiO_2 samples prior to the ALE experiments. UHP N_2 was used to blow off the samples prior to use. Prior to the silicon oxidation experiment, the native oxide on the SOI wafer was removed by wet etching. This wet etching was accomplished by dipping for 1 min in a 1:50 aqueous HF solution followed by rinsing in deionized water.

The dose valves for the reactants and the N_2 carrier gas were closed, and the gate valve before the pump was shut simultaneously to achieve static exposures. The static exposures were then conducted for various times. The reported reactant pressures refer to their partial pressures with respect to the background N_2 gas pressure of 1 Torr.

Si ALE of ultrathin silicon films was examined using a Si (100) SOI wafer with an initial thickness of approximately 100 Å. This ultrathin silicon film was obtained by thinning a silicon SOI wafer with an initial silicon thickness of 100 nm. The silicon film thickness was progressively decreased by oxidation with H_2O at 1100 °C followed by the subsequent stripping of the oxide in a dilute HF solution.^{44,45}

III. RESULTS AND DISCUSSION

1. SiO_2 ALE Using TMA and HF. Thermal SiO_2 ALE was performed to establish a baseline for the Si ALE studies. Figure 4 displays the SiO_2 thickness versus the number of SiO_2 ALE

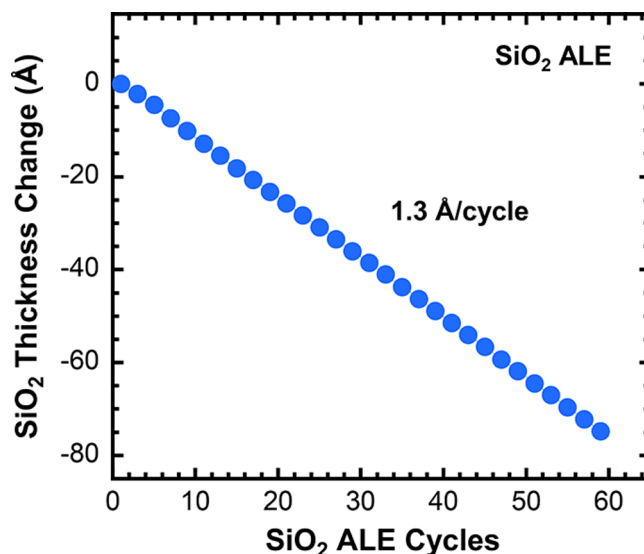


Figure 4. SiO_2 thickness change vs the number of SiO_2 ALE cycles during SiO_2 ALE using sequential TMA and HF exposures at 290 °C.

cycles measured by *in situ* spectroscopic ellipsometry (SE) at 290 °C. This etch temperature of 290 °C was chosen to avoid potential problems with TMA decomposition that may occur at higher temperatures.⁴⁶ The results in Figure 4 were obtained using sequential static exposures of TMA and HF for 5 s at partial pressures of 1.0 Torr. The static exposures were followed by 30 s N₂ purges.

Figure 4 shows that the etching of the SiO₂ film thickness was linear. SiO₂ ALE was characterized by an etch rate of 1.3 Å/cycle. The least-squares fitting of any one data set for the SiO₂ thickness change versus the number of SiO₂ ALE cycles was accurate to ±0.001 Å/cycle. The etch rate from separate experimental results run under the same conditions was accurate to within <0.1 Å/cycle. These results for SiO₂ ALE confirm earlier investigations that revealed a linear decrease in SiO₂ film thicknesses using SiO₂ ALE with TMA and HF as the reactants at 300 °C. These earlier studies were conducted in a hot wall reactor using *ex situ* SE measurements. The SiO₂ etch rates were dependent on the reactant pressures.²⁸ A SiO₂ etch rate of 0.31 Å/cycle was obtained with TMA and HF static pressures of 4 Torr for 20 s with no N₂ background pressure during reactant exposures.²⁸

2. Si ALE Using O₂, HF, and TMA. Figure 5 shows the film thickness change for both Si and SiO₂ during Si ALE at 290 °C

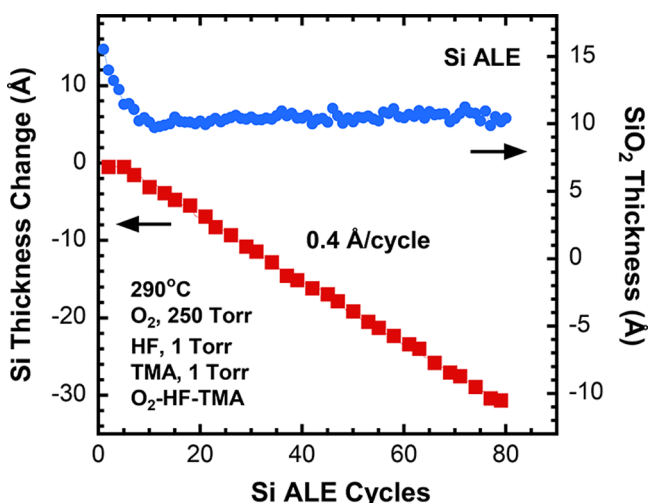


Figure 5. Si thickness change and SiO₂ film thickness vs the number of Si ALE cycles during thermal Si ALE using sequential exposures of O₂, HF, and TMA at 290 °C.

using an O₂–HF–TMA exposure sequence. The Si and SiO₂ film thicknesses were monitored simultaneously using the SE measurements. The Si ALE process utilized static reactant pressures of 250, 1.0, and 1.0 Torr and exposure times of 10, 5, and 5 s for O₂, HF, and TMA, respectively. Figure 5 shows that the Si film thickness decreases linearly with the number of Si ALE cycles. A Si etch rate of 0.4 Å/cycle is observed after a short nucleation period of two or three cycles. The least-squares fitting of any one data set for the Si thickness change versus the number of Si ALE cycles was accurate to ±0.002 Å/cycle. The etch rate from separate experimental results run under the same conditions was accurate to <0.1 Å/cycle.

During the first 10 cycles, the thickness of the SiO₂ layer decreases from an initial value of 16 Å to a final value of 10 Å. For the next 70 cycles, the SiO₂ thickness remains at 10–12 Å. Si ALE occurs at an etch rate of 0.4 Å/cycle, while the SiO₂

film thickness is essentially constant. During these cycles, the sequential Si oxidation and the SiO₂ etching processes have reached a steady state. These results are similar to the results for W ALE that were reported previously.³² W ALE occurs using an “oxidation–conversion–fluorination” etching mechanism.³²

According to Figure 1, silicon is etched by Si oxidation to SiO₂ using O₂ and the subsequent conversion of SiO₂ to Al₂O₃ using TMA.²⁸ The Al₂O₃ is then removed by fluorination and ligand-exchange reactions using HF and TMA.²⁰ On the basis of the densities of Si and SiO₂, a Si etch rate of 0.40 Å is equivalent to Si oxidation producing SiO₂ at a rate of 0.75 Å/cycle and the subsequent removal of SiO₂ at a rate of 0.75 Å/cycle. The Si etch rate of 0.40 Å/cycle also represents a silicon coverage of 2.0×10^{14} Si atoms/cm².

Figure 6 displays the results for Si ALE at various O₂ pressures. The O₂ pressures were 30, 90, 170, and 250 Torr.

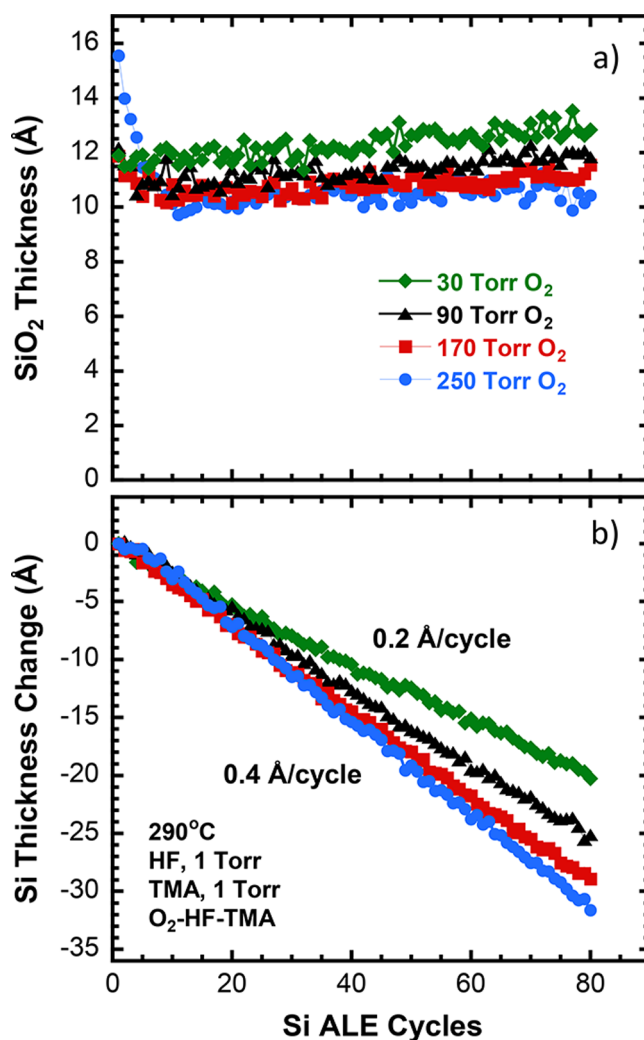


Figure 6. (a) SiO₂ thickness and (b) Si thickness change vs the number of Si ALE cycles for various O₂ pressures during Si ALE at 290 °C.

The O₂–HF–TMA exposure sequence was employed with HF and TMA partial pressures of 1.0 Torr. Static exposure times for O₂, HF, and TMA were 10, 5, and 5 s, respectively. The N₂ purge time after each static exposure was 30 s. Figure 6a shows

the thickness of the SiO₂ layer. Figure 6b displays the thickness change of the underlying Si during Si ALE.

Figure 6a reveals that the SiO₂ thicknesses vary slightly between 13 Å at 30 Torr and 10 Å at 250 Torr during Si ALE. Oxidation of Si using O₂ is a temperature- and pressure-dependent process.⁴⁷ Silicon oxidation by O₂ is described by Deal–Grove oxidation kinetics.⁴⁷ The Deal–Grove kinetics predict an increase in the level of silicon oxidation at higher O₂ pressures. The slightly larger SiO₂ thickness at the low O₂ pressure of 30 Torr is contrary to this expectation. However, silicon oxidation may become more heterogeneous at lower O₂ pressures. Two-dimensional oxide island nucleation may lead to pinholes and roughness in the SiO₂ film at thin SiO₂ thicknesses.⁴⁸ Roughness in the SiO₂ film thickness at lower O₂ pressures can then be mistaken for an “effective layer thickness” in the ellipsometry analysis.⁴⁹ The slightly higher SiO₂ thickness at 30 Torr in Figure 6a is believed to be an artifact of surface roughness. Surface roughness is discussed later in more detail in section III.6.

Figure 6b shows that the Si layer thickness is decreased linearly with the number of ALE cycles at all O₂ pressures. The Si etch rate increases from 0.2 Å/cycle at 30 Torr to 0.4 Å/cycle at 250 Torr. This trend is attributed to the increase in the level of silicon oxidation at higher O₂ pressures as expected by Deal–Grove kinetics.⁴⁷ This increase is not strictly proportional to the O₂ pressures. The increase of O₂ pressure from 30 to 90 Torr produces a significantly larger increase in Si etch rate than the increase from 170 to 250 Torr. On the basis of the results depicted in Figure 6, 250 Torr is the most effective O₂ pressure for Si ALE. The O₂ pressure of 250 Torr yields the highest Si etch rate and does not display any evidence for an increase in surface roughness that may be caused by thin SiO₂ thicknesses.

Figure 7 shows the effect of various partial pressures of TMA and HF on the Si etch rate at 290 °C. These SE measurements were obtained using an O₂–HF–TMA exposure sequence. The static exposure times for O₂, HF, and TMA were 10, 5, and 5 s, respectively, with N₂ purge times of 30 s. In Figure 7a, the partial pressures of O₂ and HF were fixed at 250 and 1.0 Torr, respectively, while the pressure of TMA was varied from 0.5 to 2.0 Torr. The Si film etch rate increases from 0.2 Å/cycle at a TMA pressure of 0.5 Torr to 0.4 Å/cycle at a TMA pressure of 1.5 Torr. A further increase in the TMA pressure from 1.5 to 2.0 Torr had a negligible effect on the Si etch rate.

Higher etch rates for SiO₂ ALE were also observed at higher TMA pressures in previous studies.²⁸ Higher TMA pressures convert more SiO₂ to Al₂O₃ because the conversion process is believed to follow kinetics similar to the Deal–Grove kinetics for silicon oxidation.⁴⁷ TMA converts SiO₂ and forms an Al₂O₃ layer on the SiO₂ surface. This Al₂O₃ layer acts as a diffusion barrier to prevent additional conversion of SiO₂ to Al₂O₃.⁴⁷ Higher TMA exposures are able to yield larger Al₂O₃ thicknesses before the Al₂O₃ layer restricts further conversion.

Figure 7b shows the Si thickness change versus the number of Si ALE cycles for the O₂ and TMA pressures fixed at 250 and 1.5 Torr, respectively, and the HF pressure varied from 0.5 to 1.5 Torr. These results show no change in silicon etch rate for the different HF partial pressures. All the HF partial pressures lead to a Si etch rate of 0.4 Å/cycle. The constant Si etch rate versus HF pressure can be attributed to the constant Al₂O₃ layer thickness on the SiO₂ film that can yield only a fixed AlF₃ layer thickness.

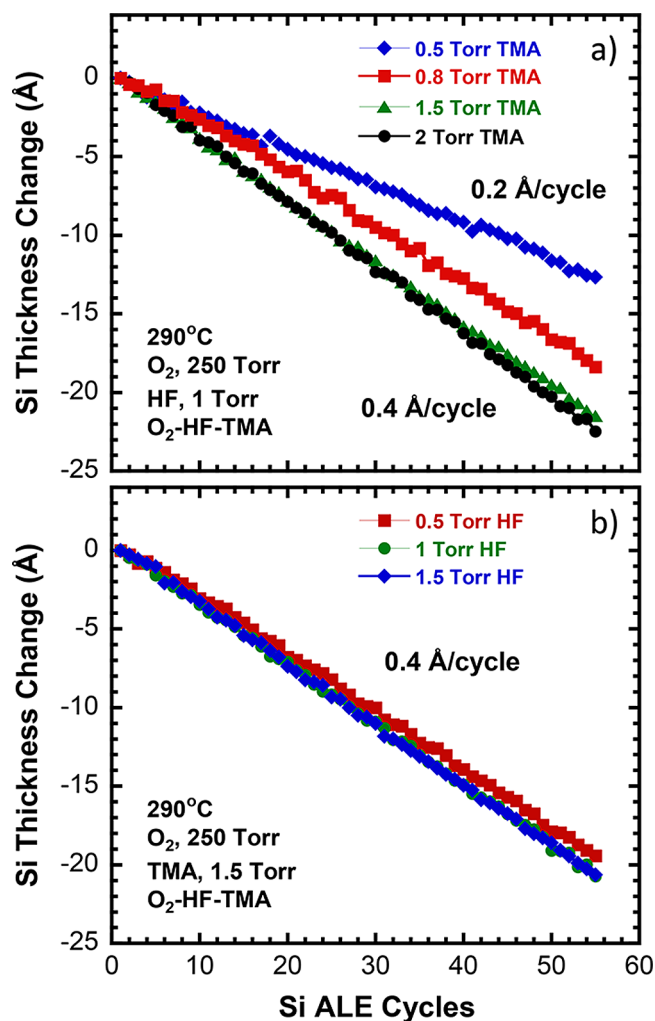


Figure 7. Si thickness change vs the number of Si ALE cycles for (a) various TMA pressures and (b) various HF pressures during Si ALE at 290 °C.

The Si etch rates versus O₂ pressure in Figure 6b are displayed in Figure 8a. The silicon etch rates versus TMA and HF pressure in panels a and b of Figure 7 are presented in panels b and c of Figure 8, respectively. These results for the Si etch rate versus O₂, TMA, and HF pressure were obtained by varying the O₂, TMA, or HF pressure while holding all the other pressures constant. The Si etch rate is observed to reach a nearly constant value in the limit of higher pressure for each reactant. This behavior is expected for self-limiting reactions that have reached saturation.

O₂ and TMA pressures increase the levels of oxidation and conversion prior to reaching saturation. Longer exposure times at a constant pressure also increase the levels of oxidation and conversion before reaching saturation. Longer O₂ exposures at a constant O₂ pressure have a negligible effect on the SiO₂ thicknesses as shown by the results in section III.5. The effect of TMA exposure time was explored by holding the exposures of O₂ and HF constant at 250 and 1.0 Torr for 10 and 5 s, respectively. At a TMA pressure of 1.0 Torr, the Si etch rate was nearly constant at longer TMA exposure times. Si etch rates of 0.26, 0.38, and 0.37 Å/cycle were measured for TMA exposure times of 2.5, 5, and 7.5 s, respectively.

3. Effect of O₂–HF–TMA versus O₂–TMA–HF Exposure Sequences. The effects of the O₂–HF–TMA and

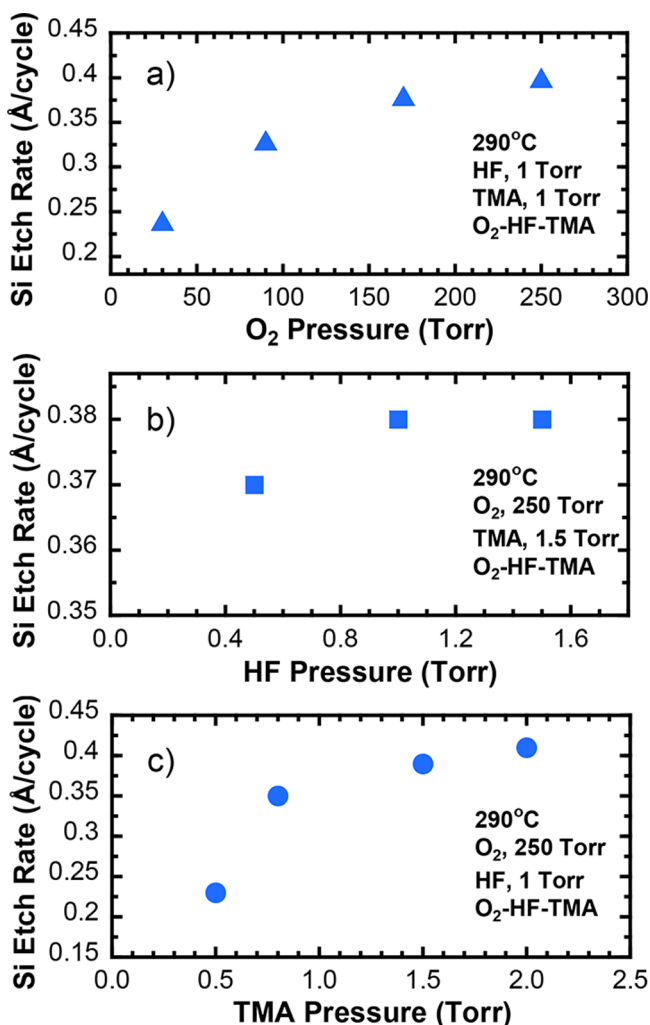


Figure 8. Si etch rate vs pressure of (a) O₂, (b) TMA, and (c) HF during Si ALE at 290 °C. Si etch rates were obtained by varying the O₂, TMA, or HF pressure while holding all other pressures constant.

O₂–TMA–HF exposure sequences on Si ALE are shown in Figure 9. These experiments were performed at 290 °C using partial pressures of O₂, HF, and TMA of 250, 1.0, and 1.0 Torr, respectively. The static exposure times for O₂, HF, and TMA were 10, 5, and 5 s, respectively, with N₂ purge times of 30 s between exposures. The results for the O₂–TMA–HF exposure sequence were obtained immediately after the O₂–HF–TMA exposure sequence.

Figure 9a shows the SiO₂ thickness during the two exposure sequences. For the O₂–HF–TMA exposure sequence, the thickness of the SiO₂ layer is decreased quickly from the native oxide thickness of 16 Å and reaches a constant thickness of 10 Å after 10 Si ALE cycles. For the O₂–TMA–HF exposure sequence, the SiO₂ thickness gradually increases from the initial oxide thickness of 11 Å remaining after the O₂–HF–TMA exposure sequence. The SiO₂ thickness reaches a constant thickness of 13 Å after 15–20 Si ALE cycles.

Figure 9b displays the Si thickness change during the O₂–HF–TMA and O₂–TMA–HF exposure sequences. The O₂–HF–TMA exposure sequence displays a Si etch rate of 0.4 Å/cycle. Switching to the O₂–TMA–HF exposure sequence decreases the Si etch rate to 0.2 Å/cycle. The different exposure sequences change the surface chemistry during Si ALE. The O₂–TMA–HF exposure sequence is believed to

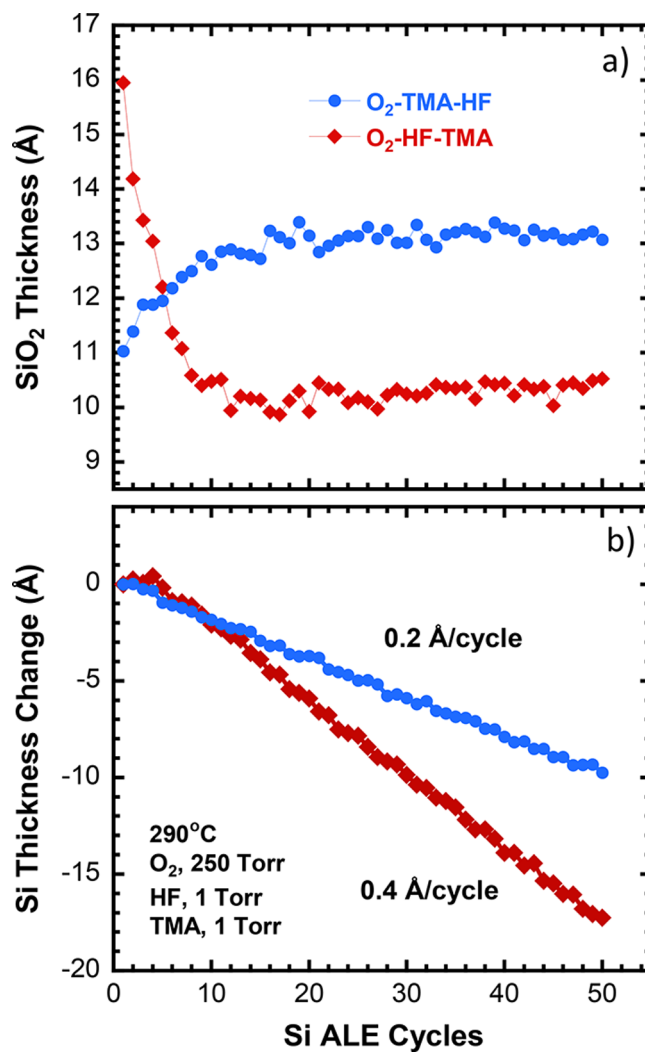


Figure 9. (a) SiO₂ thickness and (b) Si thickness change vs the number of Si ALE cycles for the O₂–HF–TMA and O₂–TMA–HF exposure sequences at 290 °C.

decrease the Si etch rate by producing additional Al₂O₃ on the surface when the TMA exposures follow the O₂ exposures. This additional surface oxide can act as a diffusion barrier and decrease the level of oxidation of the underlying silicon during the O₂ exposures and the resulting Si etch rate.

The O₂–HF–TMA exposure sequence is also more favorable because the TMA exposure occurs after the HF exposure. The HF exposure fluorinates the Al₂O₃ surface layer to produce an AlF₃ surface layer. The TMA can then undergo ligand-exchange reactions with the AlF₃ surface layer and produce volatile etch products such as AlF(CH₃)₂. For the O₂–TMA–HF exposure sequence, the O₂ exposure precedes the TMA exposure. The O₂ exposure may alter the fluorinated surface layer produced by the HF exposure. This change to the fluorinated surface layer may subsequently affect the TMA ligand-exchange reaction and decrease the Si etch rate.

The effects of the O₂ exposures and the different exposure sequences were also explored for SiO₂ ALE. Figure 10 compares the SiO₂ thickness versus the number of SiO₂ ALE cycles for the TMA–HF, O₂–HF–TMA, and O₂–TMA–HF exposure sequences at 290 °C. The partial pressures of O₂, HF, and TMA were 250, 1.0, and 1.0 Torr, respectively. Static exposure times for O₂, HF, and TMA were 10, 5, and 5 s,

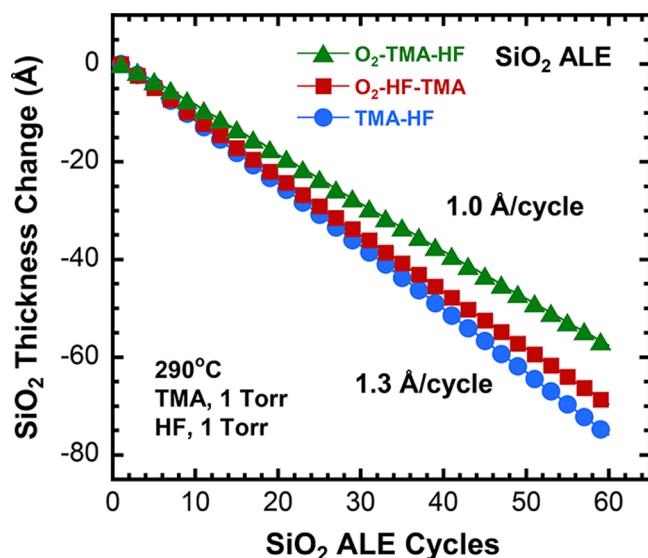


Figure 10. SiO₂ thickness change vs the number of SiO₂ ALE cycles during SiO₂ ALE using various exposure sequences at 290 °C. Exposure sequences were O₂–TMA–HF, O₂–HF–TMA, and TMA–HF.

respectively, with N₂ purge times of 30 s between exposures. The addition of the O₂ exposure to the SiO₂ ALE process decreases the SiO₂ etch rate.

Figure 10 reveals that the TMA–HF exposure sequence has a SiO₂ etch rate of 1.3 Å/cycle. The O₂–HF–TMA exposure sequence has a slightly lower SiO₂ etch rate of 1.2 Å/cycle. The O₂–TMA–HF exposure sequence has a lower SiO₂ etch rate of 1.0 Å/cycle. The SiO₂ etch process is hindered by the addition of the O₂ exposure. The O₂ exposures may be reacting with surface aluminum species to produce a thin film of Al₂O₃ that acts as a diffusion barrier and impedes the conversion of SiO₂ to Al₂O₃ by TMA. The O₂ exposure may also be leading to a change in surface species that affects the ligand-exchange reaction between TMA and the fluorinated surface. Both the oxide diffusion barrier and the change in surface species resulting from the O₂ exposure could decrease the SiO₂ etch rate.

4. Si Etch Rate versus Temperature. The Si ALE process is also dependent on the substrate temperature. Figure 11 shows the Si thickness change versus the number of Si ALE cycles at substrate temperatures of 225, 250, and 290 °C. These experiments were performed with partial pressures of O₂, HF, and TMA of 250, 1.0, and 1.0 Torr, respectively. Static exposures times for O₂, HF, and TMA were 10, 5, and 5 s, respectively. N₂ purge times of 30 s were employed between successive exposures.

A substrate temperature of 290 °C yielded a Si etch rate of 0.4 Å/cycle. Lower substrate temperatures led to a decrease in the Si etch rate. The etch rate was 0.2 Å/cycle at the lowest sample temperature of 225 °C. This temperature dependence of the Si etch rate is consistent with earlier measurements of the temperature dependence of SiO₂ ALE using TMA and HF.²⁰ This temperature dependence is likely the result of more conversion of SiO₂ to Al₂O₃ during the TMA conversion reaction at higher temperatures.

5. SiO₂ Thickness during Si Oxidation. Silicon oxidation is usually performed at temperatures and pressures much higher than the temperatures of 225–290 °C and O₂ pressures of 30–250 Torr that are employed in this study. Silicon

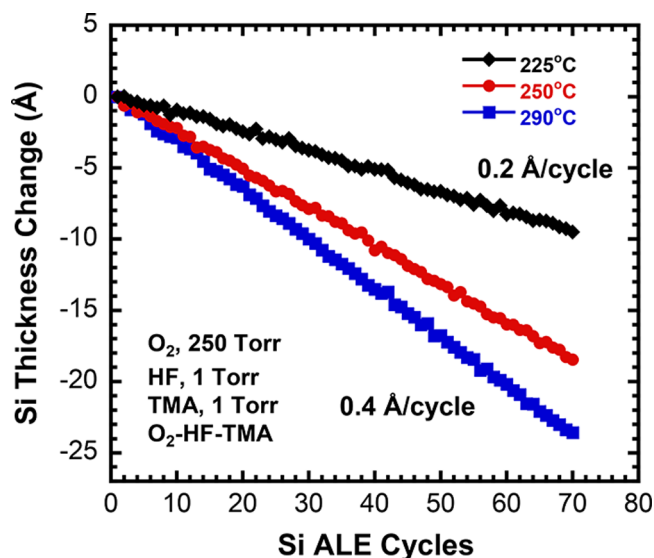


Figure 11. Si thickness change vs the number of Si ALE cycles during Si ALE at 225, 250, and 290 °C. Si ALE was performed using the O₂–HF–TMA exposure sequence.

oxidation is typically conducted at temperatures from 800 to 1000 °C at an O₂ pressure of 760 Torr.⁴⁷ To characterize silicon oxidation under the reaction conditions during Si ALE, additional experiments of silicon oxidation were performed at 290 °C and O₂ pressures of 250 Torr under the reaction conditions used for the Si ALE experiments. Figure 12 shows

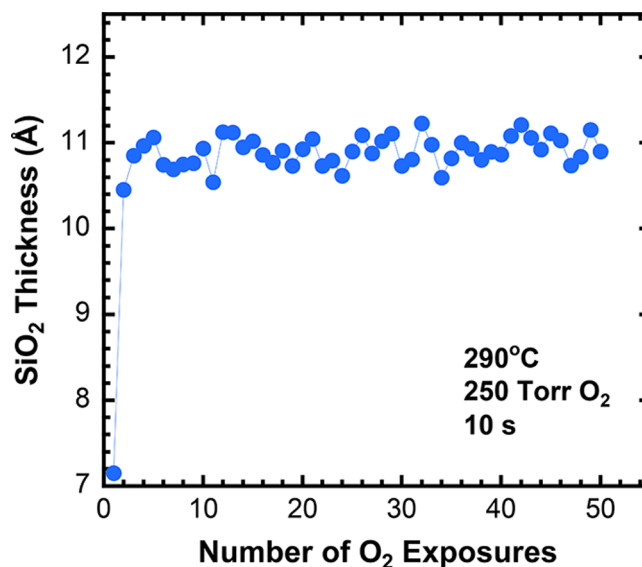


Figure 12. SiO₂ thickness vs the number of O₂ exposures at 250 Torr and 290 °C. The initial sample was a wet-etched SOI wafer.

the SiO₂ thickness on silicon versus the number of consecutive static O₂ exposures at 250 Torr for 10 s with N₂ purge times of 30 s. Prior to oxidation, the SOI wafer was wet-etched using an aqueous HF solution (1:50) to remove the native silicon oxide. The SE measurements of the SiO₂ thickness were recorded after each O₂ exposure.

Figure 12 shows that 7 Å of oxide is on the Si surface after the wet etching. This silicon oxide thickness is considered an “effective” oxide thickness and is not a real oxide thickness.⁵⁰ This “effective” oxide thickness is an artifact of the

ellipsometric measurements.^{49,50} The thickness of the effective oxide after wet etching in Figure 12 is consistent with other effective oxide thicknesses that have been observed by ellipsometry after HF wet etching of the native oxide on silicon.⁵⁰

Figure 12 reveals that the first O₂ exposure on the wet-etched SOI wafer produces a SiO₂ thickness of 10.5 Å. Subsequent oxygen exposures lead to smaller increases, and a SiO₂ thickness of 11 Å is obtained after several O₂ exposures. Similar oxidation behavior has been previously reported under comparable reaction conditions.^{51,52} At 300 °C and O₂ pressures of 1 Torr, the silicon oxidation rate has been reported to be initially high at approximately 1 Å/s. The oxidation rate was then observed to slow dramatically to 0.04 Å/s after an oxide thickness of 6 Å had been reached.⁵²

The SiO₂ thickness of 11 Å observed after several O₂ exposures in Figure 12 is also almost identical to the SiO₂ thickness of 10–11 Å observed during Si ALE in Figures 5 and 6. Figure 12 confirms that a SiO₂ thickness of 11 Å can be reached after only one O₂ exposure at 250 Torr for 10 s at 290 °C. This behavior indicates that the O₂ exposures during Si ALE are sufficient for self-limiting silicon oxidation.

A SiO₂ thickness of ~11 Å remains after Si ALE. This SiO₂ thickness can be decreased by performing SiO₂ ALE after Si ALE.²⁸ The O₂ exposure is removed from the three-step ABC process for Si ALE. SiO₂ ALE is then performed using a two-step AB process with TMA and HF without any change in reaction conditions.²⁸ Ellipsometry measurements indicate that the SiO₂ layer can be nearly completely removed from silicon using SiO₂ ALE. However, measuring these ultrathin SiO₂ thicknesses accurately with spectroscopic ellipsometry is difficult.

6. Surface Roughness versus O₂ Pressure. Atomic force microscopy (AFM) measurements were employed to compare the surface roughness of the SOI wafers before and after Si ALE. Figure 13 shows an AFM image of the SOI wafer after 100 Si ALE cycles using an O₂ pressure of 250 Torr at 290 °C. The AFM image of the as-received SOI wafer was nearly identical to the AFM image shown in Figure 13. The root-mean-square (RMS) roughness was 2.0 ± 0.2 Å for the as-received SOI wafer and for the SOI wafer after the etch process using an O₂ pressure of 250 Torr. The RMS roughness was uniform across the 2.5 cm × 2.5 cm SOI wafer.

Figure 14 shows the AFM image of the SOI wafer after 100 Si ALE cycles at an O₂ pressure of 30 Torr at 290 °C. The lower O₂ pressure of 30 Torr in the Si ALE cycle leads to an increased RMS roughness of 8.6 ± 0.3 Å. In addition, the image in Figure 14 reveals signs of porosity. This higher roughness with evidence for porosity is consistent with the higher effective SiO₂ thickness observed by the SE measurements during Si ALE at lower O₂ pressures in Figure 6a. The SiO₂ film roughness and porosity may lead to a larger effective SiO₂ thickness from the SE analysis. These observations suggest that an O₂ pressure of 30 Torr is too low for Si ALE. Higher O₂ pressures are needed to maintain adequate silicon oxidation for uniform silicon etching during Si ALE without surface roughening.

7. Si ALE of Ultrathin Si Films. Si ALE may be useful for preparing precisely controlled ultrathin silicon films that display quantum confinement effects.⁵³ Silicon quantum wells and silicon nanomembranes have displayed band gap shifts at silicon film thicknesses of <100 Å.^{54,55} Silicon in the quantum confinement regime also undergoes a change from an

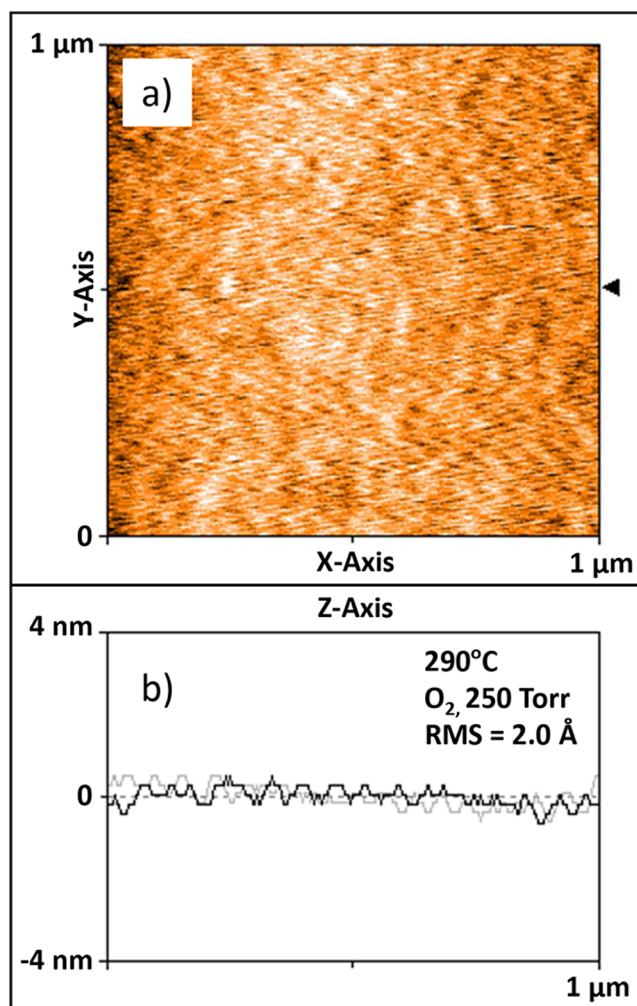


Figure 13. AFM image of the SOI wafer after 100 cycles of Si ALE using the O₂–HF–TMA exposure sequence at 290 °C with an O₂ pressure of 250 Torr. The RMS surface roughness is 2.0 ± 0.2 Å.

indirect to a direct band gap transition.^{53,56} Consequently, Si ALE could be important for silicon band gap tuning and optoelectronics applications.

Figure 15 displays the silicon thickness during Si ALE for an initial silicon film thickness of approximately 100 Å. The etching was performed using partial pressures of O₂, HF, and TMA of 250, 1.0, and 1.0 Torr, respectively. The static exposures times for O₂, HF, and TMA were 10, 5, and 5 s, respectively, with N₂ purge times of 30 s. Figure 15 shows a linear decrease in the silicon film thickness versus the number of Si ALE cycles over the entire thickness range. The etch rate was 0.5 Å/cycle from the initial silicon film thickness of approximately 100 Å until the silicon film was completely removed from the SiO₂ film on the SOI wafer.

There is a slight difference between the etch rate of 0.5 Å/cycle measured in Figure 15 and the etch rate of 0.4 Å/cycle measured in Figures 5–7 and 9 under equivalent reaction conditions. This small difference can be attributed to the different ellipsometry model used to analyze the results from the ultrathin silicon films. As mentioned in section II, B-spline (Si) was replaced with Si Temp JAW for modeling the results from the ultrathin silicon thicknesses.

There is no observation of a change in the etch rate in Figure 15 for silicon films in the quantum confinement regime

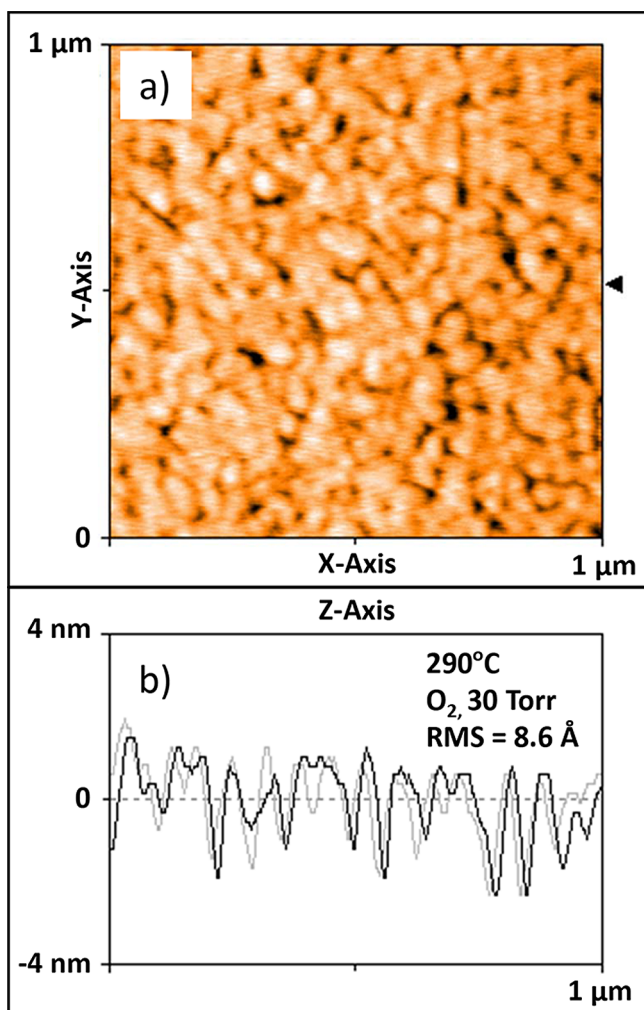


Figure 14. AFM image of the SOI wafer after 100 cycles of Si ALE using the O₂–HF–TMA exposure sequence at 290 °C with an O₂ pressure of 30 Torr. The RMS surface roughness is 8.6 ± 0.3 Å.

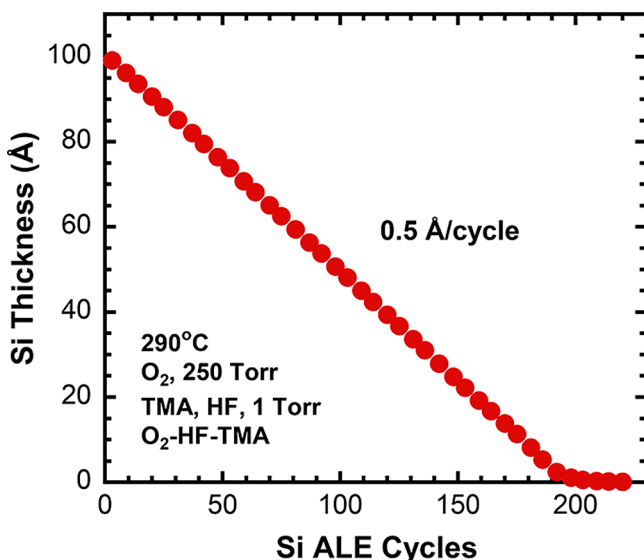


Figure 15. Si thickness vs the number of Si ALE cycles during Si ALE at 290 °C. Si ALE was performed on an ultrathin silicon film with an initial thickness of 100 Å on the SiO₂ film of an SOI wafer.

at silicon thicknesses of <100 Å.^{54,55} The optical properties of ultrathin silicon films display changes at photon energies of >3 eV in the quantum confinement regime.^{44,57} However, these changes do not affect the determination of the film thickness using spectroscopic ellipsometry.^{44,57}

The linearity of the decrease in silicon thickness with the number of Si ALE cycles displayed in Figure 15 indicates that Si ALE can produce precise ultrathin silicon thicknesses. These controlled ultrathin silicon thicknesses obtained by an isotropic etch process should be useful for advanced semiconductor fabrication.³⁷ For example, isotropic Si etching is desired for the formation of Si nanowires.⁵⁸ Thermal Si ALE could also be used for postprocessing of various Si structures used in microelectromechanical systems (MEMS) and nanoelectromechanical systems (NEMS).⁴² Ultrathin silicon thicknesses could also have applications in other silicon areas such as optoelectronics,³⁸ photonics,³⁹ flexible electronics,⁴¹ thermoelectrics,⁴⁰ and ultrathin separation membranes.⁴³ The constancy of Si ALE for silicon thicknesses of <100 Å occurs even though earlier studies have revealed difficulties with the oxidation of silicon films on SOI wafers with thicknesses of <100 Å.⁵⁹ Slower Si oxidation rates were also reported for small diameter silicon nanowires.⁶⁰

IV. CONCLUSIONS

Atomic layer controlled thermal etching of Si has been demonstrated by *in situ* SE measurements using an oxidation and “conversion-etch” mechanism. This thermal Si ALE process employs static exposures of O₂, HF, and TMA in an O₂–HF–TMA exposure sequence. The reaction conditions for thermal Si ALE at 290 °C were static reactant pressures of 250, 1.0, and 1.0 Torr and exposure times of 10, 5, and 5 s for O₂, HF, and TMA, respectively. These reaction conditions produced a Si ALE etch rate of 0.4 Å/cycle at 290 °C.

The Si ALE was dependent on the O₂ pressure, the TMA pressure, and the reactant exposure sequence. Higher O₂ and TMA pressures produced higher Si etch rates until they reached a saturation value at higher pressures. The O₂ pressure dependence results from the larger oxidation of the underlying Si film at higher O₂ pressures. The TMA pressure dependence results from more conversion of SiO₂ to Al₂O₃ at higher TMA pressures. The O₂–HF–TMA exposure sequence yielded a Si etch rate that was higher than the Si etch rate for the O₂–TMA–HF exposure sequence. The preference for the O₂–HF–TMA exposure sequence is attributed to more favorable ligand-exchange when the TMA exposures follow the HF exposures and less Al₂O₃ formation when the TMA exposures precede the O₂ exposures.

The Si ALE studies also observed the importance of adequate silicon oxidation during the O₂ exposures. For low O₂ pressures of 30 Torr, there was evidence of roughness in the SiO₂ film from the SE and AFM measurements. At higher O₂ pressures of 90–250 Torr, the SiO₂ film was very smooth. In addition, the oxidation of the SOI wafer was rapid and reached self-limiting oxidation conditions at O₂ pressures of 250 Torr for 10 s at 290 °C. The etching of ultrathin silicon films with thicknesses of <100 Å also did not display any changes resulting from possible quantum confinement effects. The ultrathin silicon films showed a linear decrease in film thickness with the number of Si ALE cycles until the silicon film was completely removed from the SiO₂ film on the SOI wafer.

■ AUTHOR INFORMATION

Corresponding Author

*E-mail: steven.george@colorado.edu.

ORCID 

Steven M. George: 0000-0003-0253-9184

Notes

The authors declare no competing financial interest.

■ ACKNOWLEDGMENTS

This research was funded by the Advanced Industries Accelerator (AIA) Program administered by the State of Colorado. Additional support was also provided by the National Science Foundation (CHE-1609554). The authors acknowledge Andrew Cavanagh at the University of Colorado and Donald David, Ken Smith, and Jim Kastengren at the CIRES/Chemistry Electronics and Mechanical shop at the University of Colorado for their help constructing the experimental apparatus. The experimental apparatus was funded by the Defense Advanced Projects Agency (DARPA) under Grant W911NF-13-1-0041.

■ REFERENCES

- (1) Kanarik, K. J.; Lill, T.; Hudson, E. A.; Sriraman, S.; Tan, S.; Marks, J.; Vahedi, V.; Gottscho, R. A. Overview of Atomic Layer Etching in the Semiconductor Industry. *J. Vac. Sci. Technol., A* **2015**, *33*, 020802.
- (2) Sakaue, H.; Iseda, S.; Asami, K.; Yamamoto, J.; Hirose, M.; Horiike, Y. Atomic Layer Controlled Digital Etching of Silicon. *Jpn. J. Appl. Phys.* **1990**, *29*, 2648–2652.
- (3) Matsuura, T.; Murota, J.; Sawada, Y.; Ohmi, T. Self-Limited Layer-by-Layer Etching of Si by Alternated Chlorine Adsorption and Ar⁺ Ion Irradiation. *Appl. Phys. Lett.* **1993**, *63*, 2803–2805.
- (4) Suzue, K.; Matsuura, T.; Murota, J.; Sawada, Y.; Ohmi, T. Substrate Orientation Dependence of Self-Limited Atomic Layer Etching of Si with Chlorine Adsorption and Low Energy Ar⁺ Irradiation. *Appl. Surf. Sci.* **1994**, *82–83*, 422–427.
- (5) Park, S. D.; Lee, D. H.; Yeom, G. Y. Atomic Layer Etching of Si(100) and Si(111) Using Cl₂ and Ar Neutral Beam. *Electrochem. Solid-State Lett.* **2005**, *8*, C106–C109.
- (6) Sugiyama, T.; Matsuura, T.; Murota, J. Atomic-Layer Etching of Ge Using an Ultraclean ECR Plasma. *Appl. Surf. Sci.* **1997**, *112*, 187–190.
- (7) Lim, W. S.; Park, S. D.; Park, B. J.; Yeom, G. Y. Atomic Layer Etching of (100)/(111) GaAs with Chlorine and Low Angle Forward Reflected Ne Neutral Beam. *Surf. Coat. Technol.* **2008**, *202*, S701–S704.
- (8) Park, S. D.; Oh, C. K.; Bae, J. W.; Yeom, G. Y.; Kim, T. W.; Song, J. I.; Jang, J. H. Atomic Layer Etching of InP Using a Low Angle Forward Reflected Ne Neutral Beam. *Appl. Phys. Lett.* **2006**, *89*, 043109.
- (9) Metzler, D.; Bruce, R. L.; Engelmann, S.; Joseph, E. A.; Oehrlein, G. S. Fluorocarbon Assisted Atomic Layer Etching of SiO₂ Using Cyclic Ar/C₄F₈ Plasma. *J. Vac. Sci. Technol., A* **2014**, *32*, 020603.
- (10) Metzler, D.; Li, C.; Engelmann, S.; Bruce, R. L.; Joseph, E. A.; Oehrlein, G. S. Fluorocarbon Assisted Atomic Layer Etching of SiO₂ and Si Using Cyclic Ar/C₄F₈ and Ar/CHF₃ Plasma. *J. Vac. Sci. Technol., A* **2016**, *34*, 01b101.
- (11) Park, J. B.; Lim, W. S.; Park, B. J.; Park, I. H.; Kim, Y. W.; Yeom, G. Y. Atomic Layer Etching of Ultra-Thin HfO₂ Film for Gate Oxide in MOSFET Devices. *J. Phys. D: Appl. Phys.* **2009**, *42*, 055202.
- (12) Park, S. D.; Lim, W. S.; Park, B. J.; Lee, H. C.; Bae, J. W.; Yeom, G. Y. Precise Depth Control and Low-Damage Atomic Layer Etching of HfO₂ using BCl₃ and Ar Neutral Beam. *Electrochem. Solid-State Lett.* **2008**, *11*, H71–H73.
- (13) Li, C.; Metzler, D.; Lai, C. S.; Hudson, E. A.; Oehrlein, G. S. Fluorocarbon Based Atomic Layer Etching of Si₃N₄ and Etching

Selectivity of SiO₂ Over Si₃N₄. *J. Vac. Sci. Technol., A* **2016**, *34*, 041307.

(14) Kim, W. H.; Sung, D.; Oh, S.; Woo, J.; Lim, S.; Lee, H.; Bent, S. F. Thermal Adsorption-Enhanced Atomic Layer Etching of Si₃N₄. *J. Vac. Sci. Technol., A* **2018**, *36*, 01b104.

(15) Kim, Y. Y.; Lim, W. S.; Park, J. B.; Yeom, G. Y. Layer by Layer Etching of the Highly Oriented Pyrolytic Graphite by Using Atomic Layer Etching. *J. Electrochem. Soc.* **2011**, *158*, D710–D714.

(16) Vogli, E.; Metzler, D.; Oehrlein, G. S. Feasibility of Atomic Layer Etching of Polymer Material Based on Sequential O₂ Exposure and Ar Low-Pressure Plasma-Etching. *Appl. Phys. Lett.* **2013**, *102*, 253105.

(17) Berry, I. L.; Kanarik, K. J.; Lill, T.; Tan, S.; Vahedi, V.; Gottscho, R. A. Applying Sputtering Theory to Directional Atomic Layer Etching. *J. Vac. Sci. Technol., A* **2018**, *36*, 01b105.

(18) Lee, Y.; George, S. M. Atomic Layer Etching of Al₂O₃ Using Sequential, Self-Limiting Thermal Reactions with Sn(acac)₂ and HF. *ACS Nano* **2015**, *9*, 2061–2070.

(19) George, S. M.; Lee, Y. Prospects for Thermal Atomic Layer Etching Using Sequential, Self-Limiting Fluorination and Ligand-Exchange Reactions. *ACS Nano* **2016**, *10*, 4889–4894.

(20) Lee, Y.; DuMont, J. W.; George, S. M. Trimethylaluminum as the Metal Precursor for the Atomic Layer Etching of Al₂O₃ Using Sequential, Self-Limiting Thermal Reactions. *Chem. Mater.* **2016**, *28*, 2994–3003.

(21) DuMont, J. W.; George, S. M. Competition Between Al₂O₃ Atomic Layer Etching and AlF₃ Atomic Layer Deposition Using Sequential Exposures of Trimethylaluminum and Hydrogen Fluoride. *J. Chem. Phys.* **2017**, *146*, 052819.

(22) Zywotko, D. R.; Faguet, J.; George, S. M. Rapid Atomic Layer Etching of Al₂O₃ Using Sequential Exposures of Hydrogen Fluoride and Trimethylaluminum with No Purging. *J. Vac. Sci. Technol., A* **2018**, *36*, 061508.

(23) Hennessy, J.; Moore, C. S.; Balasubramanian, K.; Jewell, A. D.; France, K.; Nikzad, S. Enhanced Atomic Layer Etching of Native Aluminum Oxide for Ultraviolet Optical Applications. *J. Vac. Sci. Technol., A* **2017**, *35*, 041512.

(24) Lee, Y.; DuMont, J. W.; George, S. M. Atomic Layer Etching of AlF₃ Using Sequential, Self-Limiting Thermal Reactions with Sn(acac)₂ and Hydrogen Fluoride. *J. Phys. Chem. C* **2015**, *119*, 25385–25393.

(25) Lee, Y.; DuMont, J. W.; George, S. M. Atomic Layer Etching of HfO₂ Using Sequential, Self-Limiting Thermal Reactions with Sn(acac)₂ and HF. *ECS J. Solid State Sci. Technol.* **2015**, *4*, NS013–NS022.

(26) Lee, Y.; George, S. M. Thermal Atomic Layer Etching of HfO₂ Using HF for Fluorination and TiCl₄ for Ligand-Exchange. *J. Vac. Sci. Technol., A* **2018**, *36*, 061504.

(27) Lee, Y.; Huffman, C.; George, S. M. Selectivity in Thermal Atomic Layer Etching Using Sequential, Self-Limiting Fluorination and Ligand-Exchange Reactions. *Chem. Mater.* **2016**, *28*, 7657–7665.

(28) DuMont, J. W.; Marquardt, A. E.; Cano, A. M.; George, S. M. Thermal Atomic Layer Etching of SiO₂ by a “Conversion-Etch” Mechanism Using Sequential Reactions of Trimethylaluminum and Hydrogen Fluoride. *ACS Appl. Mater. Interfaces* **2017**, *9*, 10296–10307.

(29) Zywotko, D. R.; George, S. M. Thermal Atomic Layer Etching of ZnO by a “Conversion-Etch” Mechanism Using Sequential Exposures of Hydrogen Fluoride and Trimethylaluminum. *Chem. Mater.* **2017**, *29*, 1183–1191.

(30) Lemaire, P. C.; Parsons, G. N. Thermal Selective Vapor Etching of TiO₂: Chemical Vapor Etching via WF₆ and Self-Limiting Atomic Layer Etching Using WF₆ and BCl₃. *Chem. Mater.* **2017**, *29*, 6653–6665.

(31) Lee, Y.; George, S. M. Thermal Atomic Layer Etching of Titanium Nitride Using Sequential, Self-Limiting Reactions: Oxidation to TiO₂ and Fluorination to Volatile TiF₄. *Chem. Mater.* **2017**, *29*, 8202–8210.

- (32) Johnson, N. R.; George, S. M. WO_3 and W Thermal Atomic Layer Etching Using "Conversion-Fluorination" and "Oxidation-Conversion-Fluorination" Mechanisms. *ACS Appl. Mater. Interfaces* **2017**, *9*, 34435–34447.
- (33) Xie, W. Y.; Lemaire, P. C.; Parsons, G. N. Thermally Driven Self-Limiting Atomic Layer Etching of Metallic Tungsten Using WF_6 and O_2 . *ACS Appl. Mater. Interfaces* **2018**, *10*, 9147–9154.
- (34) Johnson, N. R.; Sun, H. X.; Sharma, K.; George, S. M. Thermal Atomic Layer Etching of Crystalline Aluminum Nitride Using Sequential, Self-limiting Hydrogen Fluoride and $\text{Sn}(\text{acac})_2$ Reactions and Enhancement by H_2 and Ar Plasmas. *J. Vac. Sci. Technol., A* **2016**, *34*, 050603.
- (35) Lee, Y.; DuMont, J. W.; George, S. M. Mechanism of Thermal Al_2O_3 Atomic Layer Etching Using Sequential Reactions with $\text{Sn}(\text{acac})_2$ and HF. *Chem. Mater.* **2015**, *27*, 3648–3657.
- (36) HSC Chemistry; HSC Chemistry S.1, Outokumpu Research Oy: Pori, Finland.
- (37) Carver, C. T.; Plombon, J. J.; Romero, P. E.; Suri, S.; Tronic, T. A.; Turkot, R. B. Atomic Layer Etching: An Industry Perspective. *ECS J. Solid State Sci. Technol.* **2015**, *4*, N5005–N5009.
- (38) Fiory, A. T.; Ravindra, N. M. Light Emission From Silicon: Some Perspectives and Applications. *J. Electron. Mater.* **2003**, *32*, 1043–1051.
- (39) Thomson, D.; Zilkie, A.; Bowers, J. E.; Komljenovic, T.; Reed, G. T.; Vivien, L.; Marris-Morini, D.; Cassan, E.; Virost, L.; Fedeli, J. M.; Hartmann, J. M.; Schmid, J. H.; Xu, D. X.; Boeuf, F.; O'Brien, P.; Mashanovich, G. Z.; Nedeljkovic, M. Roadmap on Silicon Photonics. *J. Opt.* **2016**, *18*, 073003.
- (40) Hochbaum, A. I.; Chen, R. K.; Delgado, R. D.; Liang, W. J.; Garnett, E. C.; Najarian, M.; Majumdar, A.; Yang, P. D. Enhanced Thermoelectric Performance of Rough Silicon Nanowires. *Nature* **2008**, *451*, 163–167.
- (41) Kim, D. H.; Ahn, J. H.; Choi, W. M.; Kim, H. S.; Kim, T. H.; Song, J. Z.; Huang, Y. G. Y.; Liu, Z. J.; Lu, C.; Rogers, J. A. Stretchable and Foldable Silicon Integrated Circuits. *Science* **2008**, *320*, 507–511.
- (42) Waits, C. M.; Morgan, B.; Kastantin, M.; Ghodssi, R. Microfabrication of 3D Silicon MEMS Structures Using Gray-Scale Lithography and Deep Reactive Ion Etching. *Sens. Actuators, A* **2005**, *119*, 245–253.
- (43) Striemer, C. C.; Gaborski, T. R.; McGrath, J. L.; Fauchet, P. M. Charge- and Size-based Separation of Macromolecules Using Ultrathin Silicon Membranes. *Nature* **2007**, *445*, 749–753.
- (44) Price, J.; Diebold, A. C. Spectroscopic Ellipsometry Characterization of Ultrathin Silicon-on-Insulator Films. *J. Vac. Sci. Technol. B* **2006**, *24*, 2156–2159.
- (45) Tabe, M.; Kumezawa, M.; Ishikawa, Y. Quantum-Confinement Effect in Ultrathin Si Layer of Silicon-on-Insulator Substrate. *Jpn. J. Appl. Phys., Part 2* **2001**, *40*, L131–L133.
- (46) Gow, T. R.; Lin, R.; Cadwell, L. A.; Lee, F.; Backman, A. L.; Masel, R. I. Decomposition of Trimethylaluminum on Silicon(100). *Chem. Mater.* **1989**, *1*, 406–411.
- (47) Deal, B. E.; Grove, A. S. General Relationship for Thermal Oxidation of Silicon. *J. Appl. Phys.* **1965**, *36*, 3770–3778.
- (48) Watanabe, H.; Miyata, N.; Ichikawa, M. Layer-by-Layer Oxidation of Si(001) Surfaces. In *Fundamental Aspects of Silicon Oxidation*; Chabal, Y. J., Ed.; Springer Series in Materials Science; Springer: Berlin, 2001; Vol. 46, pp 89–105.
- (49) Yao, H.; Woollam, J. A.; Alterovitz, S. A. Spectroscopic Ellipsometry Studies of HF Treated Si (100) Surfaces. *Appl. Phys. Lett.* **1993**, *62*, 3324–3326.
- (50) Utani, K.; Suzuki, T.; Adachi, S. HF-Treated and NH_4OH -Treated (111)Si Surfaces Studied by Spectroscopic Ellipsometry. *J. Appl. Phys.* **1993**, *73*, 3467–3471.
- (51) Massoud, H. Z.; Plummer, J. D.; Irene, E. A. Thermal Oxidation of Silicon in Dry Oxygen Growth-Rate Enhancement in the Thin Regime 0.1. Experimental Results. *J. Electrochem. Soc.* **1985**, *132*, 2685–2693.
- (52) Enta, Y.; Mun, B. S.; Rossi, M.; Ross, P. N.; Hussain, Z.; Fadley, C. S.; Lee, K. S.; Kim, S. K. Real-Time Observation of the Dry Oxidation of the Si(100) Surface with Ambient Pressure X-ray Photoelectron Spectroscopy. *Appl. Phys. Lett.* **2008**, *92*, 012110.
- (53) Barbagiovanni, E. G.; Lockwood, D. J.; Simpson, P. J.; Goncharova, L. V. Quantum Confinement in Si and Ge Nanostructures: Theory and Experiment. *Appl. Phys. Rev.* **2014**, *1*, 011302.
- (54) Jang, H.; Lee, W.; Won, S. M.; Ryu, S. Y.; Lee, D.; Koo, J. B.; Ahn, S. D.; Yang, C. W.; Jo, M. H.; Cho, J. H.; Rogers, J. A.; Ahn, J. H. Quantum Confinement Effects in Transferrable Silicon Nanomembranes and Their Applications on Unusual Substrates. *Nano Lett.* **2013**, *13*, 5600–5607.
- (55) Lu, Z. H.; Grozea, D. Crystalline Si/SiO₂ Quantum Wells. *Appl. Phys. Lett.* **2002**, *80*, 255–257.
- (56) Lu, A. J.; Yang, X. B.; Zhang, R. Q. Electronic and Optical Properties of Single-Layered Silicon Sheets. *Solid State Commun.* **2009**, *149*, 153–155.
- (57) Diebold, A. C.; Price, J. Observation of Quantum Confinement and Quantum Size Effects. *Phys. Status Solidi A* **2008**, *205*, 896–900.
- (58) Pott, V.; Moselund, K. E.; Bouvet, D.; De Michielis, L.; Ionescu, A. M. Fabrication and Characterization of Gate-All-Around Silicon Nanowires on Bulk Silicon. *IEEE Trans. Nanotechnol.* **2008**, *7*, 733–744.
- (59) Popov, V. P.; Antonova, I. V.; Stas, V. F.; Mironova, L. V.; Gutakovskii, A. K.; Spesivtsev, E. V.; Mardegzhov, A. S.; Franzusov, A. A.; Feofanov, G. N. Properties of Extremely Thin Silicon Layer in Silicon-on-Insulator Structure Formed by Smart-Cut Technology. *Mater. Sci. Eng., B* **2000**, *73*, 82–86.
- (60) Buttner, C. C.; Zacharias, M. Retarded Oxidation of Si Nanowires. *Appl. Phys. Lett.* **2006**, *89*, 263106.